



Synthesis, Characterization and Application of Biogenic Silver Nanoparticles as Antibacterial and Antifungal Agents

Bright O. Uba ^a, Ebele L. Okoye ^b,
JaneFrances C. Anyichie ^a, Chinweike U. Dokubo ^c
and Emmanuel T. Ugwuoji ^{b*}

^a Department of Microbiology, Chukwuemeka Odumegwu Ojukwu University, P.M.B.02 Uli, Anambra State, Nigeria.

^b Department of Applied Microbiology and Brewing, Faculty of Biosciences, Nnamdi Azikiwe University, P.M.B. 5025, Awka, Anambra State, Nigeria.

^c Department of Science and Laboratory Technology, Delta State Polytechnic Ogwashi – Uku, Nigeria.

Authors' contributions

This work was carried out in collaboration among all authors. All authors contributed to the study conception and design. Authors JCA and CUD performed the experiments. Authors BOU, ELO and ETU analyzed the data. Authors BOU and ETO wrote and edited the manuscript. All authors read and approved the final manuscript.

Article Information

DOI: 10.9734/JAMB/2024/v24i3809

Open Peer Review History:

This journal follows the Advanced Open Peer Review policy. Identity of the Reviewers, Editor(s) and additional Reviewers, peer review comments, different versions of the manuscript, comments of the editors, etc are available here: <https://www.sdiarticle5.com/review-history/114671>

Original Research Article

Received: 24/01/2024

Accepted: 28/03/2024

Published: 04/04/2024

ABSTRACT

In order to provide a straightforward, affordable, and environmentally friendly process for the synthesis of metallic nanoparticles, scientists are turning to natural ways like employing plant extract in response to rising antimicrobial resistance and the desire for novel biocidal agents. In this

*Corresponding author: E-mail: et.ugwuoji@unizik.edu.ng;

study, we evaluated the efficacy of phyto-fabricated silver nanoparticles and antimicrobial agents against selected indoor bacterial and fungal strains isolated from the lecture and office rooms of Chukwuemeka Odimegwu Ojukwu University, Uli Nigeria. The indoor microorganisms were isolated, identified, and quantified using standard methods. To prepare and generate the aqueous extract employed in the biological synthesis of the silver nanoparticle, fresh soursop seeds were room dried, crushed, heated to boiling, and double filtered. The phyto-fabricated nanoparticles were centrifuged, dried and used for physicochemical characterization and antimicrobial assay. The synthesized silver nanoparticles were characterized using UV-Vis spectrophotometry, Fourier transformed Infra-Red Spectroscopy and scanning electron microscopy analyses. The antimicrobial assay was carried out using agar well diffusion method. The results revealed that *Aeromonas*, *Pseudomonas*, *Staphylococcus*, *Vibrio*, *Rhizopus*, *Aspergillus*, *Penicillium* and *Microsporum* were identified as the predominant potential indoor bacterial and fungal pathogenic strains. The characterized biogenic nanoparticles revealed the optical, spectral and morphological features unique to silver nanoparticles. Also, the antibacterial screening revealed that the highest zone of inhibition was observed against *Vibrio* sp. (27.50 ± 7.5 mm) at a concentration of $30 \mu\text{g/mL}$ while standard antifungal drug (ketoconazole) had the highest zone of inhibition of 21.0 ± 1.0 mm at $3.25 \mu\text{g/mL}$ against *Microsporum gypseum* while standard antifungal drug (ketoconazole) and Ag-NPs had the lowest zone of inhibition of 11.0 ± 1.0 mm at $15.0 \mu\text{g/mL}$ and $7.5 \mu\text{g/mL}$ against *Rhizopus* sp. and *Aspergillus flavus*, respectively. The negative control (DMSO) had no zone of inhibition on any of the potential indoor bacterial and fungal pathogenic strains. Statistically, there was significant ($P < 0.05$) inhibition of bacterial and fungal pathogenic strains among the means of treatment doses of *A. muricata* AgNPs, ciprofloxacin and ketoconazole standard antibiotics. The excellent antimicrobial inhibition of the tested indoor bacterial and fungal strains by the *A. muricata* fabricated silver nanoparticles even at MIC of $3.25 \mu\text{g/mL}$ could be exploited as biostatic and biocidal agents where there is contamination or public health risk of pathogenic indoor bacteria and fungi.

Keywords: Biocide; indoor microbe; phyto-fabrication; public health; silver nanoparticles.

1. INTRODUCTION

The public spends more than 90% of their time indoors, including in homes, businesses, and educational facilities, making indoor air quality a serious public health concern. One or more of the most significant microorganisms, such as bacteria and fungi, may contaminate the air inside buildings. It was discovered that microbial contamination, which causes allergic, respiratory, and immune-toxic disorders, accounted for around 33% of indoor air quality claims [1]. Numerous investigations on the microbiological contamination in various interiors of educational institutions have been conducted. Every day, millions of students visit the educational facilities at schools. Students' intense activity levels cause bacterial and fungal contamination of the indoor air, making schools riskier than other types of buildings. This can be attributed to the numerous students in each classroom, poor hygiene, and insufficient outdoor air supply. This danger is aggravated through frequent construction and upkeep of school buildings [2]. Due to its impact on human psyche, physical development, and academic achievement, the level of microbiological contamination in schools is a crucial factor.

Protecting human health requires the remediation of indoor settings with microbial contamination. This procedure should comprise removing any materials that have obvious or suspected microbial contamination and treating any surfaces with an antibacterial solution that will either kill the microorganisms or hinder their growth. However, there is growing concern about the use of synthetic chemicals in homes, businesses, classrooms, and other settings, and as a result, people are becoming more interested in what they consider to be "natural" alternatives [3]. The best approach in minimizing and eradicating potential indoor microbial exposure and health effects is to use antimicrobial agents of botanical origin that are generally considered nontoxic to human and public health. This therefore requires the exploration of phyt fabrication of metallic nanoparticles with antimicrobial potentials.

The consumer goods, pharmaceutical, chemical, environmental, energy, agricultural, and communication industries can all benefit from using nanoparticles, which are best described as micro molecules made through physical, chemical, physicochemical, or biological processes [4]. According to recent studies, using

plant parts like seeds, leaves, and stems to produce metallic nanoparticles is the most repeatable, affordable, and straightforward method [5]. The most significant metal nanoparticle, silver, has been found to exhibit both antibacterial and antifungal effects. Increased antibacterial properties of plant-biosynthesized silver nanoparticles have been reported in a number of literatures [6,7,8]. Silver nano compounds alone from different plant parts or in combination with antibiotics have a broad-spectrum antimicrobial activity against several pathogens like *Escherichia coli*, *S. aureus*, *Enterococcus faecium*, *Klebsiella pneumoniae*, *Salmonella typhi*, *Listeria monocytogenes*, *Acinetobacter baumannii*, *Micrococcus luteus*, *Staphylococcus epidermidis*, *Staphylococcus saprophyticus*, *Enterobacter faecalis*, *Pseudomonas aeruginosa*, *Aspergillus fumigatus*, *Penicillium notatum*, *Rhizopus stolonifer*, *Aspergillus flavus* *Trichoderma viride*, *Candida albicans* and *Candida neoformans* in previous research publications, respectively [9,10,11,12]. However, the antimicrobial potentials of *A. muricata* seed-based silver nanoparticles are less studied.

Soursop, also known as *Annona muricata*, is a plant of the Annonaceae family, order Magnoliales, and division Magnoliophyta. The soursop tree has low branches and is between 5 and 10 metres tall and 15 to 83 centimetres in diameter. It produces fruits with 55 to 170 black seeds when they are new, which become light brown when they are dry [13]. In its raw state, a soursop has 81% water, 17% carbs, 1% protein, and very little fat. Numerous medical applications have been made of *A. muricata*'s leaves, bark, fruit, and seeds. The fruit is valued not just as food but also for its juice, which is used as a galactagogue to treat liver, heart, and diarrheal illnesses [14]. The medicinal uses of *A. muricata* leaves included treatments for hypertension, diabetes [15] and cancer [16]. *A. muricata* fruit, seeds, leaves, and roots have also been employed as antimicrobials, biopesticides, bioinsecticides, and topical insect repellents [13].

There is now a wealth of information around numerous AgNPs, but little is known about their mode of action or range of antimicrobial efficacy, especially for non-clinical species. Although there are few or no studies examining the use of AgNPs against bacteria and fungi relevant to indoor air quality, the focus of this research is on the use of AgNPs as prospective antimicrobial therapies and biocides. At Chuwkuemeka Odimegwu Ojukwu University (COOU), Uli,

Nigeria, we quantified, isolated and characterized the potential indoor microorganisms from the lecture rooms and offices. We also evaluated the effectiveness of phyto-fabricated silver nanoparticles from aqueous extract of *A. muricata* against a number of indoor bacterial and fungal strains.

2. MATERIALS AND METHODS

2.1 Sample Collection and Processing

Fresh, healthy, ripe soursop fruits (*A. muricata*) were acquired at Nnobi in Anambra State, Nigeria. The fruits were then put inside a clean plastic bag and taken to the Anambra State COOU Uli Campus Microbiology Laboratory for additional processing. The fruits were cleaned, and then sliced into two pieces with a sterile knife. The seeds were then removed from the fruit, washed, and dried for 14 days at room temperature [17].

2.2 Isolation of Bacterial and Fungal Aerosol Contaminant

A settle plate method was used with 32 open 8.5 cm diameter Petri dishes holding various culture mediums according to the methods given by Badger-Emeka et al. [18] and Mora et al. [19]. By using this technique, bacteria or fungal carrying particles can settle on culture media. While fungi were isolated using Potato Dextrose Agar (PDA) and an antibacterial agent called chloramphenicol, bacteria were isolated using Nutrient Agar (NA) that had an antifungal compound called nystatin added to it. The sampling area was in the corner and middle of the chosen lecture room and the tops of the office rooms (designated as A, B, C, and D). The media plates were set on a table with the sampling height 1 m above the floor, which roughly represented the human breathing zone. The lids of eight plates were open and exposed. The plates were allowed to stay for 30 min. To ensure accurate sampling, duplicate samples for each culture medium were taken. The plates were then covered, maintained in a tightly sealed case, transported to the COOU Microbiology Laboratory, and incubated for 24 h at 37 °C. A protective gown, mouth mask, and sterile gloves were worn during the air sampling process to prevent self-contamination of the agar plates. Prior to use, the agar plates were also visually inspected for any signs of microbial growth. Using a colony counter and magnifying glass, bacterial colonies were enumerated after 24 h and fungal colonies after 5 days [20].

2.3 Sub-culture of Bacterial and Fungal Isolate

From the 32 cultivated agar plates, microbial sub-culture was used to isolate pure strains. The 32 plates' dominant colonies were sub-cultured onto 10 plates (5 NA plates and 5 PDA plates). The aseptic streak plate method was employed to perform the subculture. To do this, the NA and PDA were produced in accordance with the manufacturer's instructions, sterilized in an autoclave, cooled, and then poured into the Petri plate and allowed to solidify. Selected colonies were taken from the agar plates and streaked on fresh Petri plates using a sterile inoculating wire loop. The plates were covered with its lid gently and carefully incubated at 37 °C for 24 h while the fungal plates were incubated at 25°C for 5 days [18].

2.4 Identification of Bacterial and Fungal Isolate

Colony morphology (pigmentation, colony form, margin, and elevation), microscopy (Gram staining), and biochemical tests (oxidase, urease, methyl red, indole, citrate, motility, catalase, starch hydrolysis, and H₂S tests) were used to characterize each individual bacterial isolate, while lactophenol cotton blue staining (spores and hyphal structures) and macroscopic characteristics were used to characterize the fungal isolates. The Bergey's Manual for Determinative Bacteriology by Holt et al. [21] and the Fungus Atlas by Barnett and Hunter [22] were used to identify five bacterial and fungal isolates.

2.5 Extraction of Plant Constituent

After being dried and pulverized in a sterile ceramic mortar, the *A. muricata* seed was weighed and 25 g of the ground seed was poured to a conical flask with 100 mL of sterile deionized water. The flask was then sealed with foil and cotton wool. It was then heated using a hot plate magnetic stirrer at 70 to 80 °C for 25 minutes until a colour change was observed. Be aware that the colour shift signifies the formation of the plant extract. Conical flask was removed from hot plate magnetic stirrer after extract creation, allowed to cool, and extract was obtained by twofold filtration using muslin cloth and Whatman No 1 filter paper [17].

2.6 Biosynthesis of Silver Nanoparticles

Conical flask containing the ready-made silver nitrate (AgNO₃) solution (0.1 mM) was set on the

stirrer. The burette was fixed into the conical flask after a retort stand with a burette clamped to it was set up. On a hot plate magnetic stirrer that was calibrated to 70 °C, the solution contained in the flask was heated. A 50 mL of the seed water extract of *A. muricata* was put into a burette and dropped gradually into a solution of silver nitrate. To stop silver nitrate from being photo-reduced, the mixture was continuously swirled for one hour at 70 °C in a dark room chamber. The physical colour change from an inert solution (silver nitrate solution) to a dark brown substance (Ag/AgCl NPs) was used to demonstrate the bio-reduction of Ag⁺ to Ag⁰. The nanoparticles were centrifuged (7800 x g, 20 min, 25-30 °C) and the sediments were washed twice with deionized water and oven-dried overnight [12]. Until usage, the nanoparticles were kept at room temperature in a cool, dry cupboard.

2.7 Characterization of the Silver Nanoparticles

The generated biogenic silver nanoparticles were characterized using UV-visible spectroscopy at wavelengths between 200 and 800 nm and visible colour change determination. By using an X-ray diffractometer, the phase purity and crystalline nature were determined. Using scanning electron microscopy, the generated NPs' sizes and morphologies were determined (SEM). The functional groups of the synthesized NPs were determined using Fourier transform infrared (FTIR) spectroscopy [23,24].

2.8 Antimicrobial Assay

By employing the well diffusion method and Muller Hinto Agar (MHA) and Potato Dextrose Agar, antimicrobial properties of the biosynthesized AgNPs were examined against indoor bacteria and fungi (PDA). A stock solution of Ag-NPs comprising 60 mg/mL was created using 3% dimethylsulfoxide (DMSO) solution for the antibacterial assay. Ag-NPs stock solution was diluted twice serially in four test tubes to produce the following concentrations: 30 mg/mL, 15 mg/mL, 7.5 mg/mL, and 3.25 mg/mL. Similarly, a 2-fold dilution of positive control (ciprofloxacin) was prepared to obtain four concentrations of the antibiotic with the DMSO as negative control. To obtain fresh microorganisms, the ten indoor microbial test cultures were inoculated in Nutrient Broth (Himedia) and Potato Dextrose Broth (Himedia) and incubated for 24 h at 37 ± 0.1°C and 72 h at

25°C for the bacteria and fungi, respectively. Muller Hinton Agar (Himedia) and Potato Dextrose Agar (Himedia) were sterilized at 121 °C and 15 psi² for 15 min and later dispensed into clean sterile Petri dishes under aseptic condition until the agar solidified. The freshly prepared indoor microbial cultures were adjusted to 0.5 McFarland turbidity standard and the test microbes (0.1 mL) were inoculated using a sterilized swab stick on the surface of the solid medium in each of the Petri dishes. Thereafter, 10 mm diameter wells were created using sterile 10 mm cork borer in both solidified media above. Using a micropipette, 50 µL of AgNP at each concentration was dispensed into the wells. Similar process was carried out for the various concentrations of ciprofloxacin and DMSO and placed in the respective labelled wells. The set up was allowed to stand for 1 h for diffusion to take place after which the plates were inverted and incubated for 24 h at 37 ± 0.1°C for bacteria and 72 h at 25 °C for fungi. After incubation, zones of inhibition were measured from three different angles around the individual wells and recorded [17].

3. RESULTS

3.1 Indoor Microbial Profile

The result of the microbial counts from lecture rooms and office rooms (CFU/m³) is presented in Table 1. All plates were contaminated with bacteria and fungi. The office room A and lecture D had the highest and lowest bacterial counts of 7.50 x 10⁹ CFU/m³ and 0.34 x 10⁹ CFU/m³ while

Lecture Room A and office room A and D had the highest and lowest fungal counts of 3.20 x 10⁸ CFU/m³ and 0.38 x 10⁸ CFU/m³, respectively. The colonial morphological (Table 2), biochemical and microscopic (Table 3) characteristics of the indoor bacterial strains have been presented. Table 2 showed the colonial pigmentation, form, margin and elevation and indicated that most bacterial strains were whitish, irregular, undulate and raised. On aggregate, Table 3 indicated that the bacterial strains were positive to methyl red (100%), oxidase (60%), urease (100%), indole (100%), citrate (100%), catalase (100%), motility (100%), hydrogen sulphide (100%), fructose (80%) and sucrose (80%), tests while negative to starch hydrolysis (100%) and glucose (100%), tests. The isolates were more Gram negative (60%) and less Gram positive (40%). The bacterial isolates were, thus, identified as *Aeromonas* sp. (20%), *Pseudomonas aeruginosa* (20%), *Staphylococcus aureus* (40%), and *Vibrio* sp. (20%). The results of the macroscopic (Tables 4) and microscopic (Table 5) characteristics of the indoor fungal strains have been presented. The tables indicates that most (40%) of the fungal strains were *Aspergillus* sp. (*A. flavus* and *A. niger*) with cottony to powdery texture, whitish black to green colonial surfaces, septate hyaline hyphae and smooth to rough conidiophores. Other fungal strains identified were *Rhizopus* sp., *Penicillium* sp., *Microsporium gypseum*. The microbial strains were designated as IBA, IBB, IBC, IBD, IBE, IFA, IFB, IFC, IFD and IFE, respectively.

Table 1. Microbial counts from lecture rooms and office rooms (CFU/m³)

Sampling location	Bacterial count (x 10 ⁹ CFU/m ³)	Fungal count (x 10 ⁸ CFU/m ³)
Office room A	7.50	0.38
Office room B	1.30	0.60
Office room C	3.60	0.51
Office room D	3.40	0.38
Lecture Room A	1.30	3.20
Lecture Room B	1.70	3.10
Lecture Room C	1.80	1.40
Lecture Room D	0.34	1.10

Key: CFU/m³ = Colony forming unit per cubic metre

Table 2. Colonial morphological characteristics of the indoor bacterial isolates

Isolate Code	Pigmentation	Colony Form	Colony margin	Elevation
IBA	White cloudy	Irregular	Undulate	Raised
IBB	Lightly yellow	Irregular	Undulate	Raised
IBC	Brownish white	Irregular	Undulate	Raised
IBD	White	Irregular	Undulate	Raised
IBE	White cloudy	Irregular	Undulate	Raised

Table 3. Biochemical and microscopic characteristics of the indoor bacterial strains

Parameter	Bacterial strain code				
	IBA	IBB	IBC	IBD	IBE
Methyl red	+	+	+	+	+
Oxidase	+	+	-	-	+
Urease	+	+	+	+	+
Indole	+	+	+	+	+
Citrate	+	+	+	+	+
Catalase	+	+	+	+	+
Motility	+	+	+	+	+
Starch hydrolysis	-	-	-	-	-
Hydrogen sulphide	+	+	+	+	+
Fructose	-	+	+	+	+
Glucose	-	-	-	-	-
Sucrose	-	+	+	+	+
Gram reaction	Gram negative	Gram negative	Gram Positive	Gram positive	Gram negative
Shape	Straight rod	Rod	Cocci	Cocci	Short curve rod
Arrangement	Single, pairs	Single	Cluster	Cluster	Clustered, single
Identity	<i>Aeromonas</i> sp.	<i>Pseudomonas aeruginosa</i>	<i>Staphylococcus aureus</i>	<i>Staphylococcus aureus</i>	<i>Vibrio</i> sp.

Note: + = positive; - = negative

Table 4. Macroscopic characteristics of the indoor fungal strains

Isolate code	Reverse colony tint	Texture	Surface colony tint
IFA	Pale white	Deeply cottony	Gray-black older colony
IFB	Pale yellow	Cottony	Whitish-black
IFC	Creamy	Powdery	Whitish green
IFD	Whitish yellow	Velvety to powdery	White
IFE	Yellow	Powdery to granular	Cinnamon brown

Table 5. Microscopic features of the indoor fungal strains

Isolate code	Microscopic feature	Identity
IFA	Presence of rhizoid, round black sporangia, long branched hyphae and unbranched sporangiophores	<i>Rhizopus</i> sp.
IFB	Smooth brown coloured conidiophore and conidia. The conidiophores are protrusions from a septate and hyaline hypha and are biseriate.	<i>Aspergillus niger</i>
IFC	Colourless and rough textured conidiophores with septate tiny hyphae containing hyaline and both uniseriate and biseriate.	<i>Aspergillus flavus</i>
IFD	Branched unicellular conidia with clustered phialides and bluish-green colour. Branching, septate hyphae with hyaline.	<i>Penicillium</i> sp.
IFE	Thin and rough walled macroconidia, broad septate hyphae with pointed ends. Club – shaped microconidia	<i>Microsporium gypseum</i>

3.2 Silver Nanoparticles Spectral Profile

The changing colour of the mix (plant extract plus AgNO₃ solution) takes place from pale brown to

dark brown colour, while colour change was also observed in the plant extract. The pale brown to dark brown indicates biosynthesis of AgNPs. The result of the absorbance spectral profile of the

synthesized silver nanoparticles is shown in Fig. 1. From the figure, the highest UV- Visible peak was found at 340 nm at absorbance of 0.876 while the lowest UV- Visible peak was found at 720 nm at absorbance of 0.098. The result of the FTIR spectral profile of *A. muricata* seeds silver-nanoparticles is shown in Fig. 2. From the figure, the highest transmitter was found at 3668.566 cm^{-1} at the peak area of 47.45837, and the lowest transmittance was found at 1050.146 cm^{-1} at the

peak of 21.4948. The results of the phase purity and crystalline characteristics (Table 6), XRD pattern and profile (Fig. 3) and scanning electron micrograph (Fig. 4) of the green synthesized silver nanoparticles are shown. From the results, there are ten peak numbers ranging from 8.5541 to 68.8359 2θ with percentage relative intensities from 1.22 to 2.09 %, respectively. There were also irregular shaped with granulated compact powder and brighter facets.

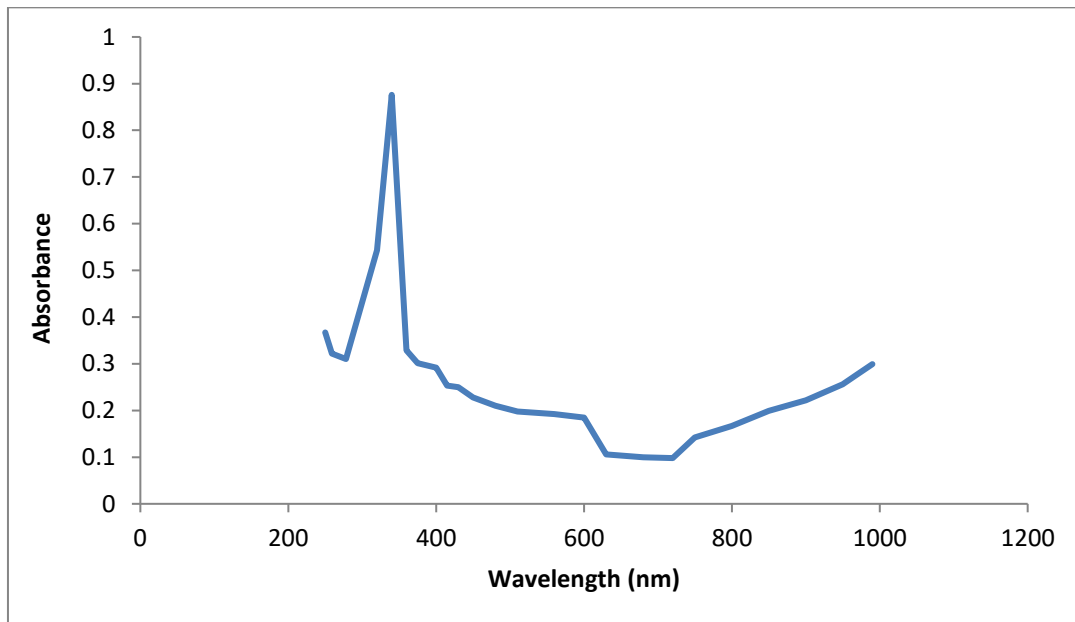


Fig. 1. UV – Vis Absorbance spectral profile of silver nanoparticle
Key: nm = nanometre

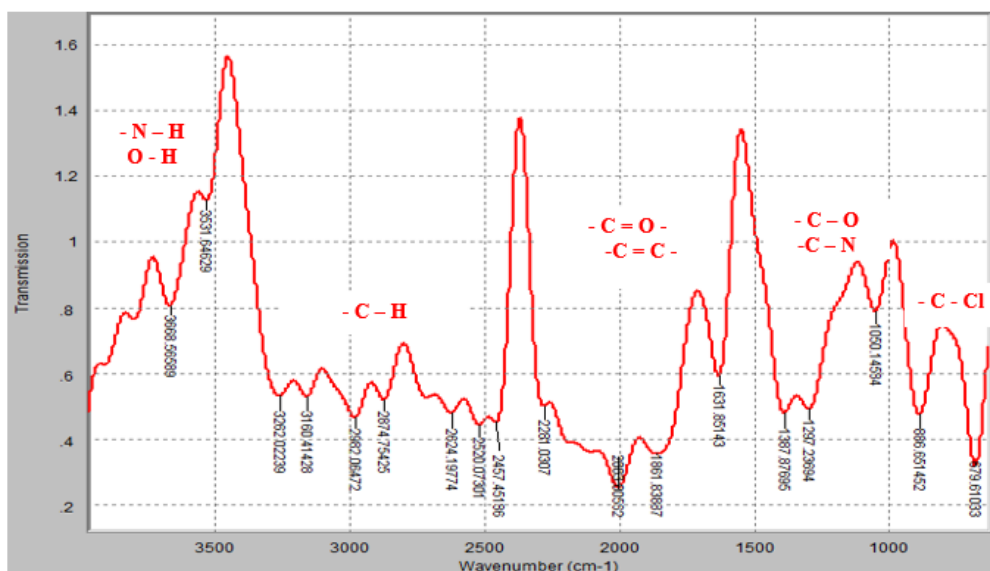


Fig. 2. FTIR spectral profile of biosynthesized silver nanoparticles
Key: cm^{-1} = Centimetre

Table 6. Phase purity and crystalline characteristics of the green synthesized silver nanoparticles

Peak no	Pos. [°2Th.]	Height [cts]	FWHM Left [°2Th.]	d-spacing [Å]	Rel. Int. [%]
1	8.5541	6.85	0.9446	10.33709	1.22
2	27.6707	10.55	0.4723	3.22389	1.88
3	32.1136	20.54	0.3936	2.78729	3.67
4	34.2501	84.74	0.1574	2.61816	15.13
5	38.0544	560.06	0.1378	2.36471	100.00
6	39.8185	14.72	0.2362	2.26393	2.63
7	44.2916	89.96	0.1968	2.04512	16.06
8	57.3933	3.42	0.9446	1.60554	0.61
9	64.5287	29.06	0.3149	1.44417	5.19
10	68.8359	11.73	0.3149	1.36395	2.09

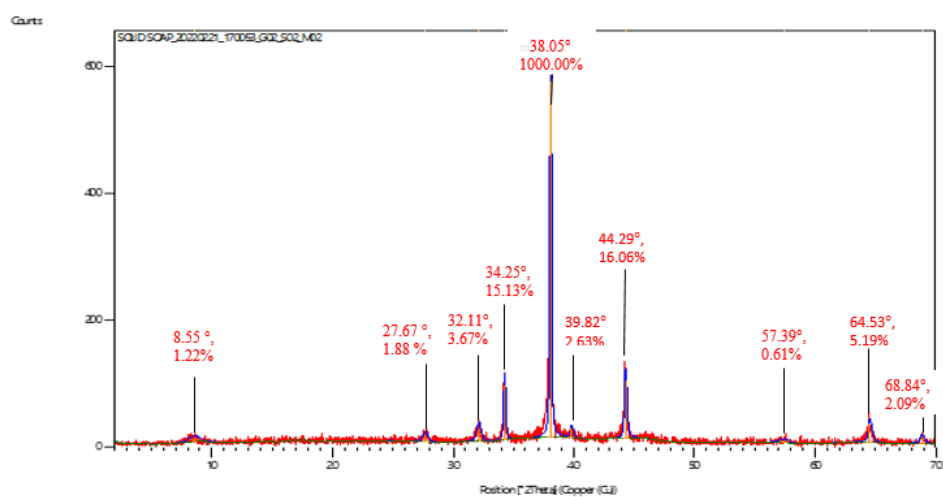


Fig. 3. XRD profile pattern of the biosynthesized AgNPs



Fig. 4. Scanning electron microphotograph of the biosynthesized silver nanoparticle (1500x magnification)

Table 7. Antibacterial effect of the Ag-NPs extracted from *Annona muricata* seeds and the standard drug (ciprofloxacin)

Isolate Identity	<i>A. muricata</i> seeds Ag-NPs				Ciprofloxacin				DMSO (Negative control)
	30 mg/mL	15 mg/mL	7.5 mg/mL	3.25 mg/mL	30 mg/mL	15 mg/mL	7.5 mg/mL	3.25 mg/mL	
<i>Aeromonas</i> sp.	21.50 ± 1.5*	14.50 ± 0.5*	15.50 ± 0.5*	19.50 ± 0.5*	17.50 ± 0.5*	15.00 ± 0.0*	14.00 ± 1.0**	10.50 ± 0.5**	0.00 ± 0.0
<i>Pseudomonas</i> sp.	16.50 ± 0.5*	16.00 ± 1.0*	16.50 ± 1.5*	16.00 ± 2.0*	16.00 ± 1.0*	15.00 ± 0.0*	13.00 ± 1.0**	10.50 ± 0.5**	0.00 ± 0.0
<i>Staphylococcus aureus</i>	18.00 ± 1.0*	15.00 ± 0.0*	14.00 ± 0.0*	11.00 ± 0.0*	15.00 ± 0.0*	16.50 ± 0.5*	14.50 ± 0.5**	10.50 ± 0.5**	0.00 ± 0.0
<i>Staphylococcus aureus</i>	19.00 ± 1.0*	20.00 ± 0.0*	17.00 ± 1.0*	22.50 ± 2.5*	20.50 ± 0.5*	19.50 ± 0.5*	18.00 ± 0.0**	16.50 ± 0.5**	0.00 ± 0.0
<i>Vibrio</i> sp.	27.50 ± 7.5*	18.00 ± 0.0*	16.50 ± 0.5*	07.50 ± 0.5*	20.00 ± 0.0*	18.50 ± 0.5*	17.00 ± 1.0**	15.00 ± 0.0**	0.00 ± 0.0

Key: Ag-NPs = Silver nanoparticles; mg/mL = Milligram per milliliter; DMSO = Dimethylsulfoxide; Results are expressed as mean value ± standard error in mean; * = Treatment mean do not differ significantly ($p > 0.05$) from each other at 95 % confidence interval; ** = Treatment mean differ significantly ($p < 0.05$) from each other at 95 % confidence interval

Table 8. Antifungal effect of the Ag-NPs extracted from *Annona muricata* seeds and the standard drug (ketoconazole)

Isolate Identity	<i>A. muricata</i> seeds Ag-NPs				Ketoconazole				DMSO (Negative control)
	30 µg/mL	15 µg/mL	7.5 µg/mL	3.25 µg/mL	30 µg/mL	15 µg/mL	7.5 µg/mL	3.25 µg/mL	
<i>Rhizopus</i> sp.	17.50 ± 1.5*	12.50 ± 1.5*	13.50 ± 1.5*	19.00 ± 1.0**	15.00 ± 0.0*	11.50 ± 1.5*	11.00 ± 1.0**	15.50 ± 0.5**	0.00 ± 0.0
<i>Aspergillus niger</i>	17.00 ± 2.0*	16.50 ± 0.5*	14.50 ± 0.5*	17.50 ± 0.5**	17.50 ± 2.5*	18.00 ± 1.0*	15.00 ± 0.0**	19.50 ± 0.5**	0.00 ± 0.0
<i>A. flavus</i>	17.50 ± 1.0*	11.00 ± 1.0*	11.00 ± 1.0*	17.50 ± 0.5**	13.00 ± 1.0*	11.00 ± 1.0*	15.50 ± 0.5**	18.50 ± 0.5**	0.00 ± 0.0
<i>Penicillium</i> sp.	15.50 ± 1.0*	20.00 ± 1.0*	15.50 ± 0.5*	19.50 ± 0.5**	18.00 ± 1.0*	15.00 ± 0.0*	17.50 ± 2.5**	19.50 ± 0.5**	0.00 ± 0.0
<i>Microsporium gypseum</i>	12.00 ± 1.0*	15.00 ± 1.0*	15.00 ± 1.0*	19.00 ± 1.0**	17.50 ± 1.5*	14.50 ± 1.5*	15.50 ± 1.5**	21.00 ± 1.0**	0.00 ± 0.0

N.B: Ag-NPs = Silver nanoparticles; mg/mL = Milligram per milliliter; DMSO = Dimethylsulfoxide; Results are expressed as as mean value ± standard error in mean; * = Treatment mean do not differ significantly ($p > 0.05$) from each other at 95 % confidence interval; ** = Treatment mean differ significantly ($p < 0.05$) from each other at 95 % confidence interval

3.3 Antimicrobial Profile

The result of the antibacterial effect of the Ag-NPs extracted from *A. muricata* seeds and the standard drug (ciprofloxacin) is summarized in Table 6. From the result, the highest zone of inhibition was observed against *Vibrio* sp. (27.50 ± 7.5 mm) at a concentration of 30 $\mu\text{g/mL}$. The lowest zone of inhibition (7.50 ± 0.5 mm) was also recorded against the same isolate and at the same concentration of the silver nanoparticle. The result of the antifungal effect of the Ag-NPs extracted from *Annona muricata* seeds and the standard drug (ketoconazole) is summarized in Table 7. From the result, standard antifungal drug (ketoconazole) had the highest zone of inhibition of 21.0 ± 1.0 mm at 3.25 $\mu\text{g/mL}$ against *Microsporium gypseum* while standard antifungal drug (ketoconazole) and Ag-NPs had the lowest zone of inhibition of 11.0 ± 1.0 mm at 15.0 $\mu\text{g/mL}$ and 7.5 $\mu\text{g/mL}$ against *Rhizopus* sp. and *Aspergillus flavus*. The negative DMSO control has no zone of inhibition on any of the indoor bacterial or fungal strains.

4. DISCUSSION

The antimicrobial efficacy of biogenic AgNPs against ten prevalent environmental air bacteria and fungi was investigated in this exploratory work. The biogenic AgNPs demonstrated broad spectrum antibacterial and antifungal activity against all ten environmental species. In this study, five bacterial and fungal isolates each were selected from various indoor sampling areas (lecture halls and office rooms) within the premises of Chukwuemeka Odumegwu Ojukwu University (COOU) Uli Campus. In comparison to lecture rooms, office rooms had a higher bacterial count (7.5×10^9 CFU/m³) and fungal count (3.20×10^8 CFU/m³). Bacterial isolates IBA, IBB and IBE were identified as *Aeromonas* sp., *Pseudomonas* sp. and *Vibrio* sp. whereas isolates IBC and IBD were identified as *Staphylococcus* spp. The five most predominant fungal isolates were selected and were finally identified as *Rhizopus* sp. IFA, *Aspergillus niger* IFB, *Aspergillus flavus* IFC, *Penicillium* sp. IFD and *Microsporium gypseum* IFE. Similar finding was published by Schroder et al. [25] who reported that the five fungal species identified were; *Aspergillus* sp., *Ulocladium* sp., *Coprinellus* sp., and two isolates of *Penicillium* sp. and they represent the most common environmental saprophytes encountered in indoor and outdoor air. Abdel – Aziz and Radwan [1] reported that their indoor analyses revealed

that the concentration of bacteria was higher than counts of fungi. In general, Gram-positive bacteria, *Bacillus*, *Micrococci* and *Staphylococci* were the predominant bacterial strains in the schools under their study and this is not in line with the observation made in this study. However, similar to our observation, they reported that the fungal flora isolated from indoor air of sampled schools showed dominant species like *Aspergillus* species, *Penicillium* species and *Alternaria* species. These findings suggest that the indoor environment in the lecture rooms and office rooms is heavily contaminated with bacteria and fungi, which could pose a potential health risk to individuals working or studying in these spaces. The identification of specific bacterial and fungal strains can help in the implementation of targeted strategies for their control and prevention. The results also highlight the importance of regular monitoring and maintenance of indoor air quality to promote a healthy and safe environment.

The result in Figs. 1 and 2 depicts the absorbance peak maximal as well as the Fourier transformed infra-red spectroscopy of the biosynthesized silver nanoparticles. The peak observation (0.876 at 340 nm) in this study could be as a result of excitation of surface plasmon resonance of metal and plant extract constituents. Previous studies by Okaiyeto et al. [8] reported similar absorbance peak wavelength range of 290 to 360 nm. Furthermore, a peak band of vibration frequencies of 679.6103 cm^{-1} and 886.6515 cm^{-1} corresponds to C - Cl (alkyl halides) stretching, while the vibration frequencies of 1050.146 cm^{-1} , 1297.237 cm^{-1} , and 1387.877 cm^{-1} corresponds to C - O (ethers group) and C - N (Amine group) group stretching. Also, the peak band of 1631.851 cm^{-1} , 1861.839 cm^{-1} , 2003.006 cm^{-1} and 2457.452 cm^{-1} corresponds to C = O (Carbonyl group) stretching. The vibration frequencies of 2520.073 cm^{-1} , 2624.198 cm^{-1} , 2874.754 cm^{-1} , 2982.065 cm^{-1} , 3160.414 cm^{-1} and 3262.022 cm^{-1} corresponds to C - H (hydrocarbyl group) stretching and finally the vibration frequencies of 3531.646 cm^{-1} and 3668.566 cm^{-1} corresponds to N - H (Amine and Hydroxyl groups) stretching. These diversities of functional groups as the components of the biosynthesized nanoparticles act as a capping, stabilizing and reducing agents [8]. The results in Table 6 and Fig. 3 revealed the main peaks are at (2θ) angles 8.55, 27.67, 32.11, 34.25, 38.05, 39.82, 44.29, 57.39, 64.53 and 68.84 by comparing JCPDS Cards No. 00-004-0783 and No. 00-041-1402). All diffraction peaks

correspond to the characteristic face centered cubic (FCC), the typical pattern of AgNPs [8;26]. Also, the crystallite grain size of the biosynthesized particle ranged from 8.81 - 31.96 nm with an average size 17.89 nm using Scherrer equation. Previous studies by Uba and Genevieve [27], Okafor et al. [28] and Rajput et al. [29] reported that the average size of the AgNPs synthesized was approximate to be ~ 50 and 13 nm, respectively which is obtained using similar formula. The result in Fig. 4 depicts that the irregular shaped granulated compact powder and brighter facets micrographic descriptions obtained in this study is in line with the observation made by previous studies carried out by Rajput et al. [29] and Shittu and Ihebunna [30]. Generally, these findings provide important insights into the physicochemical properties of the biosynthesized silver nanoparticles and pave the way for future studies in this field.

Silver is known to exhibit broad-spectrum antimicrobial activity, including bactericidal and fungicidal activity [31]. This is due to its small loss of optical frequency during surface plasmon propagation, non-toxicity, high electrical and thermal conductivity, and stability under ambient conditions. In this study, the results presented in Tables 7 and 8 indicated increased the antimicrobial activities of *A. muricata* AgNPs (7.50 – 27.50 mm and 11.00 – 19.50 mm), ciprofloxacin (10.50 – 20.50 mm) and ketoconazole (11.00 – 21.00 mm) standard antibiotics as their concentrations (3.25 µg/mL – 30.00 µg/mL) increased on the tested bacterial and fungal strains after 24 – 72 hr study period. The *Vibrio* sp. was the most and least inhibited of the tested five bacterial strains. The *Microsporum gypseum* was the most inhibited while the *Rhizopus* sp. and *Aspergillus flavus* were the least inhibited of the fungal strains. Statistically, there was significant ($P < 0.05$) inhibition among the means of *A. muricata* AgNPs, ciprofloxacin and ketoconazole treatment doses on the tested bacterial and fungal strains but significant ($p > 0.05$) was not detected only in the means of *A. muricata* AgNPs treatment doses on the tested bacterial strains. The possible reason for these significant inhibitions by *A. muricata* AgNPs could be attributed to the adhesion of their larger surface area to the tested bacterial and fungal strains leading to inhibition of numerous physiological and biochemical processes such as disturbing cell-wall permeability and cellular respiration in the cell, and subsequent destruction of the tested microbial cells [11,12]. These observations are consistent with previous

reports that have demonstrated the potential of silver nanoparticles as antimicrobial agents [32,33]. The high surface area to volume ratio and unique properties of silver nanoparticles, such as their ability to generate reactive oxygen species, have been identified as key factors contributing to their antimicrobial activity [8,33,34].

In the current study, the silver nanoparticles produced higher inhibition zones against the tested bacteria and fungi than the standard antibiotic ciprofloxacin. This finding is in contrast to a previous report by Okaiyeto et al. [8] who observed higher inhibition zone diameters from the standard antibiotic compared to the nanoparticles. The difference in results could be attributed to the nature of the plant extracts used in the two studies. Okaiyeto et al [8] used water extract of *O. genistifolia* leaves whereas water extract of *A. muricata* seed, which has reportedly high antimicrobial properties [35], was used in this study. The results of this study, thus, provide further evidence for the potential of silver nanoparticles as effective antibacterial agent, particularly when used at higher concentrations.

In a similar study by Alananbeh et al. [36], the authors investigated the effect of silver nanoparticles on the growth of four fungal strains; *Penicillium chrysogenum*, *Aspergillus niger*, *Aspergillus flavus* and then *Rhizopus* sp. and found a gradual reduction in growth as the concentration of the nanoparticles increased. Similarly, Gao et al. [37] reported successful application of different shapes and concentrations of silver nanoparticles against various fungal strains, including *Fusarium*, *Aspergillus* and *Alternaria alternate*. The results showed high inhibition, highlighting the potential of silver nanoparticles as antifungal substances. However, the antifungal activity of the biosynthesized AgNPs in this study was found to be lower compared to the positive control ketoconazole. This could be attributed to the use of crude plant extracts in the synthesis of the Ag/AgNPs instead of pure compounds. Therefore, the results of this study also suggest that biosynthesized Ag/AgNPs could potentially be used as antifungal agent, but more considerations need to be taken into account.

5. CONCLUSIONS

The findings of this study indicated that fungi and bacteria were present in the examined indoor environments. The identified microorganisms are

potential public health pathogens of concerns. The synthesis of silver nanoparticles using *A. muricata* seed is inexpensive and environmentally friendly. The silver nanoparticles displayed significant antimicrobial activities against the prevalent environmental air bacteria and fungi and therefore could be recommended as possible biocide where there is contamination or public health risk of indoor bacteria and fungi. However, further studies are needed to optimize AgNPs synthesis and to investigate the potential of AgNPs in out-door settings and their safety for human and environmental health.

ACKNOWLEDGEMENTS

The authors wish to thank the staff of Springboard Research Laboratory, Awka, Nigeria for their technical support towards the completion of this study.

COMPETING INTERESTS

Authors have declared that no competing interests exist.

REFERENCES

1. Abdel-Aziz RAZ, Radwan SM. Microbial pollution of indoor air in Riyadh city government schools. *World J Adv Res Rev.* 2020;8(1):209 – 216.
2. Nascimento PP, Alves C, Guennadievna EM Nunes T. Indoor air quality in elementary schools of Lisbon in spring. *Environmental and Geochemical Health.* 2010;33:455–468.
3. Schrodera T, Gaskin S, Ross K, Whiley H. Antifungal activity of essential oils against fungi isolated from air. *International Journal of Occupational and Environmental Health.* 2017;23(3):181–186.
4. Thakkar KN, Mhatre SS, Parikh RY. Biological synthesis of metallic nanoparticles. *Nanomedicine: Nanotechnology, Biology and Medicine.* 2010;6(2):257–262.
5. Kalaiarasi R, Jayallakshmi N, Venkatachalam P. Plant cell biotechnology. *Molecular Biology.* 2010;11: 1 –16.
6. Ahmed S, Saifullah AM, Swami BL, Ikram S. Green synthesis of silver nanoparticles using *Azadirachta indica* aqueous leaf extract. *Journal of Radiation Research and Applied Science.* 2016;9:1–7.
7. Ramesh AV, Devi DR, Battu GR and Basavaiah KA. Facile plant mediated synthesis of silver nanoparticles using an aqueous leaf extract of *Ficus hispida* Linn. f. for catalytic, antioxidant and antibacterial applications. *South African Journal of Chemical Engineering.* 2018;26:25–34.
8. Okaiyeto K, Ojemaye MO, Hoppe H, Mabinya LV, Okoh AI. Phytofabrication of silver/silver chloride nanoparticles using aqueous leaf extract of *Oedera genistifolia*: Characterization and antibacterial potential. *Molecules.* 2019;24:4382–4396.
9. Wang C, Huang X, Deng W, Chang C, Hang R, Tang B. A nano-silver composite based on the ion-exchange response for the intelligent antibacterial applications. *Material Science and Engineering C.* 2014; 41:134 – 141.
10. Salunke GR, Ghosh S, Santosh KRJ, Khade S, Vashisth P, Kale T, Chopade S, Pruthi V, Kundu G, Bellare JR. Rapid efficient synthesis and characterization of silver, gold, and bimetallic nanoparticles from the medicinal plant *Plumbago zeylanica* and their application in biofilm control. *International Journal of Nanomedicine.* 2014;9:2635–2653.
11. Ekundayo EA, Adegbenro A, Ekundayo FO, Onipede H, Bello OO, Anuoluwa IA. Antimicrobial activities of microbially synthesized silver nanoparticles against selected clinical pathogens in Akure, Nigeria. *African Journal of Microbiology Research.* 2021;15(3):132–145. Available:https://doi.org/10.5897/AJMR2020.9401
12. Helmy A, El-Shazly M, Seleem A, Abdelmohsen U, Salem M, Samir A, Rabeh M, Elshamy A and Singab ANB. The synergistic effect of biosynthesized silver nanoparticles from a combined extract of parsley, corn silk, and gum arabic: in vivo antioxidant, anti-inflammatory and antimicrobial activities. *Material Research Express.* 2020;7: 025002. Available:https://doi.org/10.1088/2053-1591/ab6e2d
13. Coria-Te´llez AV, Montalvo-Go´nzalez E, Elhadi MY, Obledo-Va´zquez EN. *Annona muricata*: A comprehensive review on its traditional medicinal uses, phytochemicals, pharmacological activities, mechanisms of action and toxicity. *Arabian Journal of Chemistry.* 2018;11:662–691.

14. Hajdu Z, Hohmann J. An ethnopharmacological survey of the traditional medicine utilized in the community of Porvenir, Bajo Paraguay Indian Reservation, Bolivia. *Journal of Ethnopharmacology*. 2012;139(3):838-857.
15. Ezuruike UF, Prieto JM. The use of plants in the traditional management of diabetes in Nigeria: Pharmacological and toxicological considerations. *Journal of Ethnopharmacology*. 2014;155(2):857-924.
16. Alonso-Castro AJ, Villarreal ML, Salazar-Olivo L, Gomez- Sanchez M, Dominguez F, Garcia-Carranca A. Mexican medicinal plants used for cancer treatment: Pharmacological, phytochemical and ethnobotanical studies. *Journal of Ethnopharmacology*. 2011;133:945–972.
17. Rotimi L, Ojemaye MO, Okoh OO, Sadimenko A, Okoh AI. Synthesis, characterization, antimalarial, antitypanocidal and antimicrobial properties of gold nanoparticle. *Green Chemistry Letters and Reviews*. 2019; 12(1):61–68.
18. Badger-Emeka LI, Al-Sultan AA, Al-Dehailan HS, Al-Humini NK, Al-Najja FA, Al-Farhan HM Potential pathogenic bacterial contaminants of shared utility devices in a University setting at Al-Hofuf, Saudi-Arabia. *African Journal of Microbiology Research*. 2015; 9(41): 2139–2144.
19. Mora M, Mahnert A, Koskinen K, Pausan MR, Oberauner-Wappis L, Krause R. Microorganisms in confined habitats: Microbial monitoring and control of intensive care units, operating rooms, cleanrooms and the international space station. *Frontiers in Microbiology*. 2016;7: 1573.
20. Sheik GB, Abd Al Rheam AI, Al Shehri ZS, Al Otaibi OM. Assessment of bacteria and fungi in air from college of applied medical sciences (Male) at AD-Dawadmi, Saudi Arabia. *International Research Journal of Biological Science*. 2015;4(9):48–53.
21. Holt JG, Kreig NR, Sneath PHA, Staley JT, Williams ST. *Bergey's manual of determinative bacteriology*. 9th edn. Maryland (USA): A Waverly Company; 1994.
22. Barnett HL, Hunter BB. *Illustrated genera of imperfect fungi*. American Phytopathology Society. 1998;2:234
23. Wang T, Jin X, Chen Z, Megharaj M, Naidu R. Green synthesis of Fe nanoparticles using eucalyptus leaf extracts for treatment of eutrophic wastewater. *Science of the Total Environment*. 2014;210:466–467.
24. Fazlzadeh M, Rahmani K, Zarei A, Abdoallahzadeh H, Nasiri F, Khosravi R. A novel green synthesis of zero valent iron nanoparticles (NZVI) using three plant extracts and their efficient application for removal of Cr (VI) from aqueous solutions. *Advanced Powder Technology Article in Press*; 2016. Available:<http://dx.doi.org/10.1016/j.apt.2016.09.003>
25. Schrodera T, Gaskin S, Ross K, Whiley H. Antifungal activity of essential oils against fungi isolated from air. *International Journal of Occupational and Environmental Health*. 2017;23(3):181 – 186.
26. Kamal A, Zaki S, Shokry H, Abd-El-Haleem D. Using ginger extract for synthesis of metallic nanoparticles and their applications in water treatment. *Journal of Pure and Applied Microbiology*. 2020;14(2):1227–1236. Available:<https://doi.org/10.22207/JPAM.14.2.17>
27. Uba BO, Obiefuna GO. Aerobically enhanced nanobioremediation of diesel oil contaminated soil and water using mycosynthesized silver nanoparticle as biostimulating agent. *Science World Journal*. 2023;18(1):75–82.
28. Okafor CA, Uba BO, Dokubo CU. Application of myco-fabricated silver nanoparticle in the adsorption of malachite green and trypan blue from aqueous solution. *Nigerian Journal of Life Sciences*. 2023;12(2):8–15. Available:<https://doi.org/10.52417/njls.v12i2.354>
29. Rajput K, Agrawal S, Sharma J, Agrawal P. Mycosynthesis of silver nanoparticles using endophytic fungus and investigation of its antibacterial and azo dye degradation efficacy *Pestalotiopsis versicolor*. *KAVAKA*. 2017;49:65–71.
30. Shittu KO, and Ihebunna O. Purification of simulated waste water using green synthesized silver nanoparticles of *Piliostigma thonningii* aqueous leave extract. *Advanced National Science: Nanoscience Nanotechnology*. 2017;8: 045003.
31. Chouhan N, Ameta R, Meena RK. Biogenic silver nanoparticles from *Trachyspermum ammi* (Ajwain) seeds extract for catalytic reduction of p-

- nitrophenol to p -aminophenol in excess of NaBH₄. Journal of Molecular Liquid. 2017; 230:74–84.
32. Yonathan K, Mann R, Mahbub KR, Gunawan C. The impact of silver nanoparticles on microbial communities and antibiotic resistance determinants in the environment. Environmental Pollution. 2022;293(2022):118506. Available:https://doi.org/10.1016/j.envpol.2021.118506.
33. Durán N, Durán M, de Jesus MB, Seabra AB, Fávaro WJ, & Nakazato G. Silver nanoparticles: A new view on mechanistic aspects on antimicrobial activity. Nanomedicine: Nanotechnology, Biology, and Medicine. 2016;12(3):789–799. Available:https://doi.org/10.1016/j.nano.2015.11.016
34. Naganthran A, Verasoundarapandian G, Khalid FE, Masarudin MJ, Zulkharnain A, Nawawi NM, Karim M, Che Abdullah CA, Ahmad SA. Synthesis, characterization and biomedical application of silver nanoparticles. Materials (Basel, Switzerland). 2022;15(2):427. Available:https://doi.org/10.3390/ma15020427
35. Abdel-Rahman T, Hussein AS, Beshir S, Hamed AR, Ali E, El-Tanany SS. Antimicrobial activity of terpenoids extracted from *Annona muricata* seeds and its endophytic *Aspergillus niger* Strain SH3 either singly or in combination. Macedonian Journal of Medical Sciences, 2019;7(19):3127–3131. Available:https://doi.org/10.3889/oamjms.2019.793
36. Alananbeh KM, Al-Refae WJ, Al-Qodah Z. Antifungal effect of silver nanoparticles on selected fungi isolated from raw and waste water. International Journal of Pharmaceutical Science. 2017; 79(4): 559–567.
37. Gao C, Xu Y, Xu C. *In vitro* activity of nano-silver against ocular pathogenic fungi. Life Science Journal. 2012;9: 750-753.

© Copyright (2024): Author(s). The licensee is the journal publisher. This is an Open Access article distributed under the terms of the Creative Commons Attribution License (<http://creativecommons.org/licenses/by/4.0>), which permits unrestricted use, distribution, and reproduction in any medium, provided the original work is properly cited.

Peer-review history:

The peer review history for this paper can be accessed here:
<https://www.sdiarticle5.com/review-history/114671>